Mansoura Engineering Journal

Volume 32 | Issue 3 Article 3

9-1-2021

Load Characteristics Effect on Dynamic Voltage Stability Analysis in HVDC Systems.

I. Bedir
Tanta University, faculty of Engineering, Tanta, Egypt.

A. Lotfy
Arab Academy for Science & Technology & Maritime Transport, Alexandria, Egypt.

G. Aly
Tanta University, faculty of Engineering, Tanta, Egypt

Recommended Citation

Bedir, I.; Lotfy, A.; and Aly, G. (2021) "Load Characteristics Effect on Dynamic Voltage Stability Analysis in HVDC Systems.," *Mansoura Engineering Journal*: Vol. 32 : Iss. 3 , Article 3.
Available at: https://doi.org/10.21608/bfemu.2007.128691

LOAD CHARACTERISTICS EFFECT ON DYNAMIC VOLTAGE STABILITY ANALYSIS IN HVDC SYSTEMS

تأثير خصائص الحمل على تحليل إستقرار الجهد الديناميكي في نظم الجهد الفائق المستمر

I. Bedir[1] A. A. Lotfy[2] G.E.M. Aly[1]

1 Tanta University, faculty of Engineering, Tanta, Egypt.
2 Arab Academy for Science &Technology & Maritime Transport, Alexandria, Egypt.

ملخص. تقدم هذه الورقه البحثيه طريقه جديده لتحليل تأثيرنموذج الحمل على إستقرار الجهد في نظم الجهد الفائق المستمر عند طرفي الموحد و العاكس. و قد تم أخذ التغيرات الديناميكيه لنظم التيار المستمر و المتحكمات في الإعتبار عند مختلف ظروف التشغيل. و قد تم تطبيق و إستخدام نموذج الإشاره الصغيره للإتزان للتعرف على حدود إتزان النظام في حالة وجود الحمل الإستاتيكي والديناميكي . كما تم حساب متغيرات نظم التيار المستمر و المتردد عند النسب المختلفة للقصر الفعال لبيان تأثر إستقرار النظام. و قد تم التحقق من النتائج بإستخدام المحاكاه الغير خطيه.

Abstract: The modeling of loads has a significant effect on the accuracy of dynamic voltage stability analysis of HVDC system. This paper investigates the dynamic nature of voltage instability considering static and dynamic load models. The load effect at different control modes of HVDC system is considered for different configurations of single infeed HVDC systems at different effective short circuit ratios. The results are validated using nonlinear simulations.

Keywords: Load Characteristics, HVDC, SIF, SIFAC, Bifurcations.

I. INTRODUCTION

The concept of voltage instability have been observed in AC systems when operating close to its steady state stability limit, also the voltage stability is related to special load locations. Converter terminals used for HVDC system can be seen as a special load which may cause voltage instability [1].

Different configurations of HVDC systems are used today at different places around the world [2]. The main configurations of HVDC systems are single-infeed (SIF) [3,5,6], single-infeed with a parallel AC line (SIFAC) [3,7] and multi-infeed systems [7,9].

Several researchers tackled the voltage instability problem for SIF [3-6], other researches developed these techniques to be suitable for SIFAC [3,7]. A static analysis of SIF considering static load effect was given in [3,4]. In the dynamic analysis given in [6] a simple representation of DC line and a simple RL circuit were considered for only two control modes. In [5] a model suitable for SIF systems sensitivity analysis was given, nevertheless, power flow effect and load power at converter bus were not considered through stability study.

In this paper, a detailed model of SIF and SIFAC systems incorporating static and dynamic load models is introduced. Nonlinear simulation is used to validate model results.

SYMBOLS:

$CESCR_{Inv}$, $CESCR_{Rect}$	Critical effective short circuit ratio for both rectifier and inverter, respectively.
CC,Cβ, CDA, CP, CDV	Constant current, constant beta, constant delay angle, constant power and constant DC voltage controllers, respectively.
Δx_{c1} and Δx_{c2}	Output of integral branch of PI Controller for both rectifier and inverter, respectively
α and β	Rectifier firing and inverter advance angles, respectively
δ_1, δ_2	Rectifier and inverter bus phase angles.
P_{d1}, P_{d2}, Q_{d1}, Q_{d2}	DC line active power transfers and reactive power consumed at rectifier and inverter side, respectively.
P_{Sr}, P_{Si}, Q_{Sr}, Q_{Si}	Active and reactive static load power at rectifier and inverter, respectively.
n_{pv}, n_{qv}	Active/reactive voltage dependent power order.
K_{pc}, k_{qc}	The active and reactive power load constants.
K_{pv}, k_{qv}	Voltage dependent active and reactive load constants.
K_{pi}, k_{qi}	The current active and reactive load constants.
K_{pz}, k_{qz}	Impedance active and reactive load constants.
P_{Lr}, P_{Li}, Q_{Lr}, Q_{Li}	Active and reactive dynamic load power at both rectifier and inverter, respectively.
FL, CL, ZL, VL	Fixed, constant current, impedance, and voltage dependent loads, respectively.

Accepted September 11, 2007

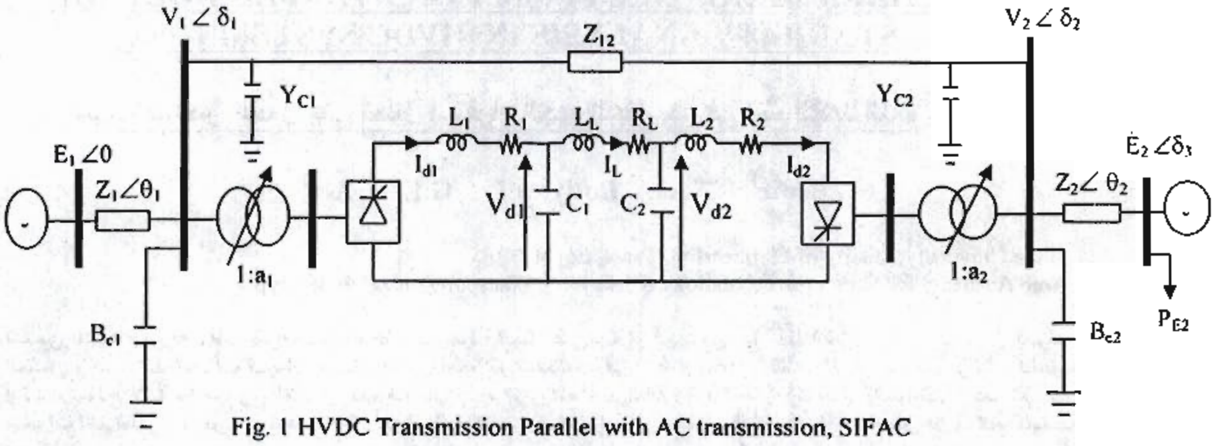

Fig. 1 HVDC Transmission Parallel with AC transmission, SIFAC

II. SYSTEM MODEL

The HVDC system for both SIF and SIFAC consists of the following parts:

1. DC System Model

The DC network includes converters (rectifier and inverter), smoothing reactors and DC transmission line. The DC transmission line is represented by its π–equivalent. The DC network is shown in the middle of Fig. 1. The DC system and DC controller differential equations are similar to that presented in [4, 8].

2. AC System Model

The active and reactive power flow through AC lines in both rectifier and inverter for SIF can be written as follows:

$$P_{acj} = V_j^2 Y_j \cos\theta_j + V_j E_j Y_{jE} \cos(\theta_{jE} - \delta_j)$$
$$Q_{acj} = -V_j^2 Y_j \sin\theta_j - V_j E_j Y_{jE} \sin(\theta_{jE} - \delta_j) \qquad (1)$$

Where; $\overline{Y}_j = 1/\overline{Z}_j + jB_{C\,j} = Y_j \angle\theta_j$ and $\overline{Y}_{jE} = 1/\overline{Z}_j = Y_{jE}\angle\theta_{jE}$,

$\overline{Z}_j = R_j + jX_j$

j =1 for rectifier and 2 for inverter.

3. AC-DC Power Flow equations

a) No load at converter buses

The system algebraic equations for SIF can be written as follows:

$$P_{ac1} + P_{d1} = 0$$
$$P_{ac2} - P_{d2} = 0 \qquad (2)$$

$$Q_{ac1} + Q_{d1} = 0$$
$$Q_{ac2} + Q_{d2} = 0 \qquad (3)$$

Equations (2) and (3) can be replaced by equations (4) and (5) to be suitable for SIFAC:

$$P_{ac1} + P_{d1} + P_{12} = 0$$
$$P_{ac2} - P_{d2} + P_{21} = 0 \qquad (4)$$
$$P_{ac3} + P_{E2} = 0$$

$$Q_{ac1} + Q_{d1} + Q_{12} = 0$$
$$Q_{ac2} + Q_{d2} + Q_{21} = 0 \qquad (5)$$

where;

$$P_{12} = V_1 V_2 Y_{12} \cos(\theta_{12} + \delta_2 - \delta_1) = -P_{21}$$
$$P_{ac3} = E_2^2 Y_3 \cos\theta_3 + E_2 V_2 Y_{2E} \cos(\theta_{2E} + \delta_2 - \delta_3)$$
$$Q_{12} = -V_1 V_2 Y_{12} \sin(\theta_{12} + \delta_2 - \delta_1) = -Q_{21}$$
$$\overline{Y}_{12} = -\frac{1}{\overline{Z}_{12}} = Y_{12}\angle\theta_{12} = Y_{21}\angle\theta_{21} \qquad (6)$$
$$\overline{Y}_3 = \frac{1}{\overline{Z}_2} = Y_3\angle\theta_3$$

b) Static Load at Converter Buses

In this work the general static load model presented in [3] was used to modify the stability analysis model presented in [8]. The active and reactive static load at converter bus can be taken as follows:

$$P_{S_{r,j}} = k_{pc} + k_{pi}V_j + k_{pz}V_j^2 + k_{pv}V_j^{n_{pv}}$$
$$Q_{S_{r,j}} = k_{qc} + k_{qi}V_j + k_{qz}V_j^2 + k_{qv}V_j^{n_{qv}} \qquad (7)$$

where j = 1 for rectifier and 2 for inverter.

The active and reactive static load power at rectifier and inverter are to be added to Equations (2) and (3) for SIF or to Equations (4) and (5) for SIFAC.

c) Dynamic Load

The dynamic active and reactive loads $P_{L_{r,i}}, Q_{L_{r,i}}$ are given by [6]

$$
\begin{aligned}
P_{L_i} &= \frac{1}{T_{p_{r,i}}}\left[x_{p_{r,i}} + \frac{1}{2}k_{pL}V_i^2\right] \\
Q_{L_i} &= \frac{1}{T_q}\left[x_{q_{r,i}} + \frac{1}{2}k_{qL}V_i^2\right]
\end{aligned}
\tag{8}
$$

The active and reactive load functions are respectively given by:

$$
\begin{aligned}
\dot{x}_{p_{r,i}} &= P_{S_{r,i}} - P_{L_{r,i}} \\
\dot{x}_{q_{r,i}} &= Q_{S_{r,i}} - Q_{L_{r,i}}
\end{aligned}
\tag{9}
$$

The active and reactive static and dynamic load at rectifier and inverter are to be added to Equations (2) and (3) for SIF or to Equations (4) and (5) for SIFAC.

4. Small Signal Stability Model

The system differential equations can be linearized to obtain the state space model as.

$$\dot{x}_{pc} = A\,x_{pc} + B\,u_{pc} \tag{10}$$

where:

$$x_{pc} = \left[\Delta w_{c1}, \Delta w_{c2}, \Delta I_{d1}, \Delta I_{d2}, \Delta V_{d1}, \Delta V_{d2}, \Delta I_L\right]$$

$$u_{pc} = \begin{cases} \left[\Delta\delta_1, \Delta\delta_2, \Delta V_1, \Delta V_2\right] & for\ SIF \\ \left[\Delta\delta_1, \Delta\delta_2, \Delta\delta_3, \Delta V_1, \Delta V_2\right] & for\ SIFAC \end{cases}$$

By linearizing equations (2) and (3) for SIF or (4) and (5) for SIFAC, the state space form of algebraic equations is obtained as.

$$0 = Cx_{pc} + Du_{pc} \tag{11}$$

Where, "C" and "D" are the Jacobian submatrices. Assuming that D remains nonsingular along system trajectories as the system parameters vary, then equations (10) and (11) are reduced to [3,5].

$$\dot{x}_{pc} = A'x_{pc} \tag{12}$$

Where $A' = A - BD^{-1}C$.

Equation (12) represents the small signal stability model of DAE suitable for SIF and SIFAC system. Voltage stability analysis is carried out by computing Eigenvalues of the system state matrix A'.

Most of the voltage instability problems are related to bifurcation. These bifurcations characterized by changes of Eigenvalues of the system equilibria as certain parameters change in the system. The main types of bifurcation are saddle node bifurcation (SN) which occurs when one Eigenvalue become zero and Hobf bifurcation (HP) which occurs when a pair of complex Eigenvalues cross the imaginary axis [3-4, 11-13]. The effect of voltage instability is greater at the AC bus connected to the converter operated at low short circuit ratio.

III. CASE STUDY

The data of the HVDC system used to implement the proposed technique is given in Table 1.

Table 1 AC and DC systems data (p.u.)

AC system Data (p.u.)

Bus No	E	R_c	L	R + j X	B_c
1	1.1	0.115	0.0052	0 + j0.2857	0.4
2	1.1	0.115	0.0052	0 + j0.3333	0.6
Z_{12} = 0.2 + j 0.6 p.u., $y_{c1} = y_{c2}$ = 0.01 p.u.					

DC Line Data (p.u.)

R_1	L_L	C_1	C_2
0.04462	0.000823	0.00027	0.000272

The HVDC system strength can be measured by the system effective short circuit ratio which is a parameter used to study system instability [6]:

$$ESCR_i = \frac{1}{Z_i} - B_{c_i} \tag{13}$$

CASE (a) Static Load

The static load data at rectifier and inverter are illustrated in Table 2.

Table 2 Static load data in p.u.

k_{pc}	k_{pi}	k_{pz}	k_{ps}	n_{ps}
0.1	0.02	0.02	0.02	1.5
k_{qc}	k_{qi}	k_{qz}	K_{qs}	n_{qs}
0.1	0.01	0.01	0.01	1.5

Fig. 2 illustrates the p-v nose curve due to change of active load power at inverter bus of SIF. The AC line voltage at both rectifier and inverter decrease with an increase of static active load power up to a maximum power of 2.522 p.u..

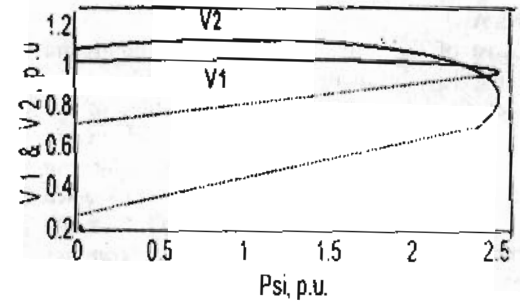

Fig. 2 The p-v nose curve at rectifier and inverter due to change of active load power at inverter (SIF adopting CC/Cβ).

Fig. 3 illustrates the p-v nose curve due to change of active load power at rectifier bus of SIFAC. The AC line voltage at both rectifier and inverter decrease with an increase of static active load power up to a maximum power of 1.031 p.u..

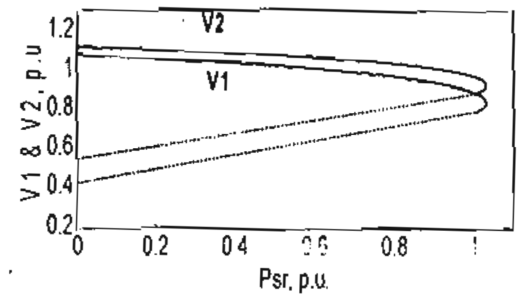

Fig. 3 The p-v nose curve at rectifier and inverter due to change of active load power at rectifier (SIFAC adopting CDA/CC).

Figs. 4 and 5 illustrate the P_{dr} against V_r and P_{dr} against I_{dr} curves at rectifier side for different types of static active and reactive loads respectively. The maximum value of DC power transfer varies according to the applied static load types. The maximum DC power transfer at different static loads is shown in Tables 3 and 4 for SIF and SIFAC, respectively.

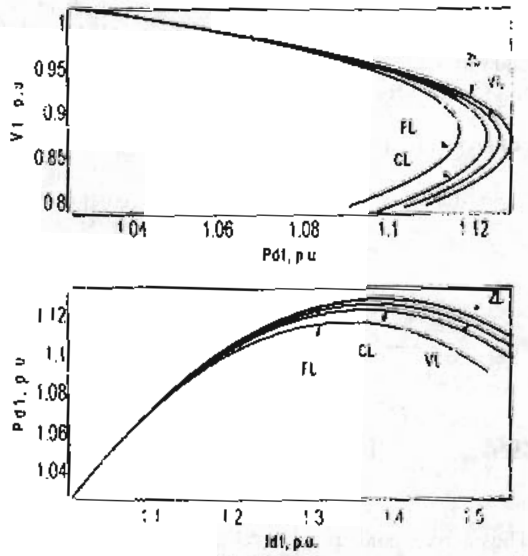

Fig. 4 The P_{dr}-V_r and P_{dr}-I_{dr} curves at rectifier at different types of static active load power (SIF adopting CDA/CC).

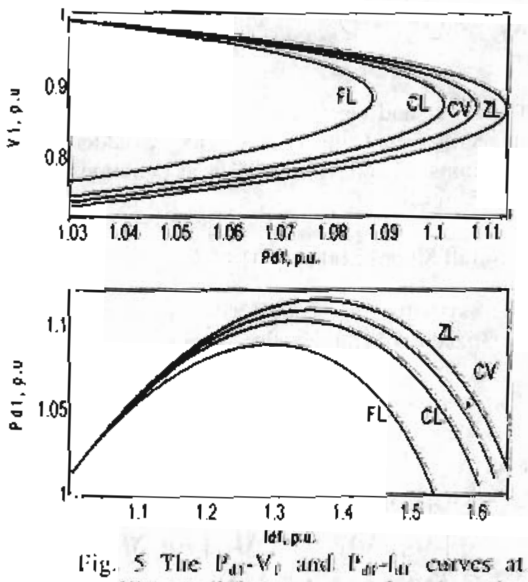

Fig. 5 The P_{dr}-V_r and P_{dr}-I_{dr} curves at rectifier at different types of static active load power (SIFAC adopting CDA/CC).

Table 3 Maximum DC Power Transfer for SIF

Load Type	Max. P_{dr} at Static Active Power Loads	Max. P_{dr} at Static Reactive Power Loads
FL	1.117	1.035
CL	1.123	1.056
ZL	1.129	1.073
VL	1.126	1.065

Table 4 Maximum DC Power Transfer for SIFAC

Load Type	Max. P_{d1} at Static Active Power Loads	Max. P_{d1} at Static Reactive Power Loads
FL	1.160	1.088
CL	1.164	1.102
ZL	1.168	1.114
VL	1.166	1.108

Fig. 6 illustrates the behavior of AC line voltage at rectifier bus versus the voltage dependent active and reactive load coefficients, at different AC line voltage dependent power orders, respectively. The system strength increases with increasing of voltage order, which must be greater than 1 [10].

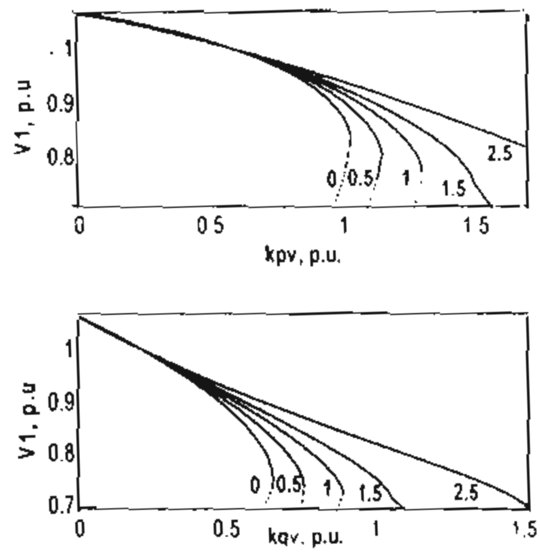

Fig. (6) AC line voltage versus the voltage dependent load coefficients for different power orders.

Reaching a critical effective short circuit ratio may be due to Saddle node (SN) or Hopf (HP) bifurcations, or power flow failure (PF). In case of load at rectifier bus, the power order coefficient of voltage dependent portion of static load positively affects the stability at this bus due to the associated reduction of this load portion. As shown in Fig 7, the effect of n_{qv} change is relatively more noticeable compared with that of n_{pv} due to the direct bearing of the reactive power on stability.

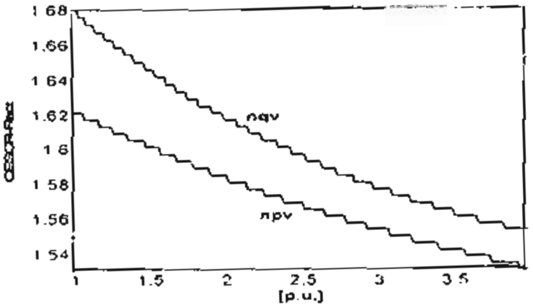

Fig. 7 CESCR$_{Rect}$ versus n_{pv1} and n_{qv1}, for CDA/CC control mode (K_{pv}, K_{qv1}=0.1)

Fig. 8 illustrates the effect of increasing k_{pc}, k_{qc}, k_{pi}, k_{qi}, k_{pz}, k_{qz}, k_{pv} and k_{qv} on CESCR$_{Rect}$. It illustrates that the CESCR$_{Rec}$ increases with an increase in either of the load constants. Nevertheless, the increase of k_{qc} and k_{pc} yielded the most significant bearing on system instability.

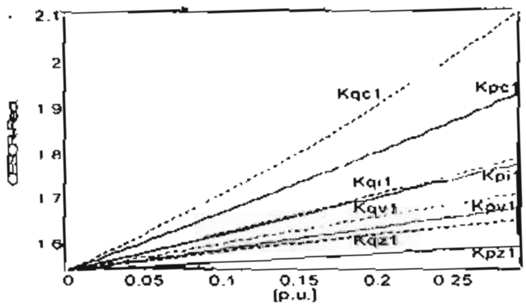

Fig. 8 CESCR$_{Rect}$ against k_{pc1}, k_{qc1}, k_{pi1}, k_{qi1}, k_{pz1}, k_{qz1}, k_{pv1} and k_{qv1} for CDA/CC

Fig. 9 shows the expected deterioration of stability at the inverter bus due to its reactive loadings. A similar loading at the rectifier bus positively affects the inverter's bus stability due to the reduction of dc power transferred and the associated reduction of reactive power needed for the commutation process. The DC line's performance is thus reduced on behalf of stability.

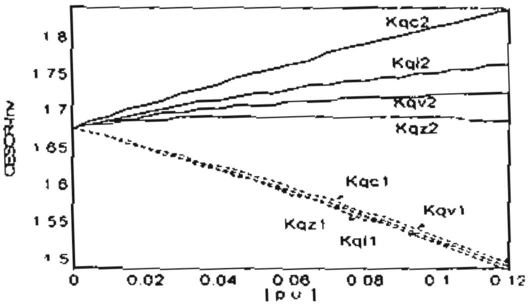

Fig. 9 CESCR$_{Inv}$ versus $k_{qc1,2}$, $k_{qi1,2}$, $k_{qz1,2}$, and $k_{qv1,2}$ for CC/Cβ control mode Load at Rectifier and Inverter bus, respectively.

Fig. 10 corresponds to an SIF stable case at SCR_{Rect} of 2.7776. The system adopts CDV/CC control mode with an increase of 0.01 p.u. in the current order of the inverter's CC controller. The rectifier current oscillates around a stable node. The responses of AC line voltages at both rectifier and inverter buses cause the shown subsequent changes in static active and reactive load power

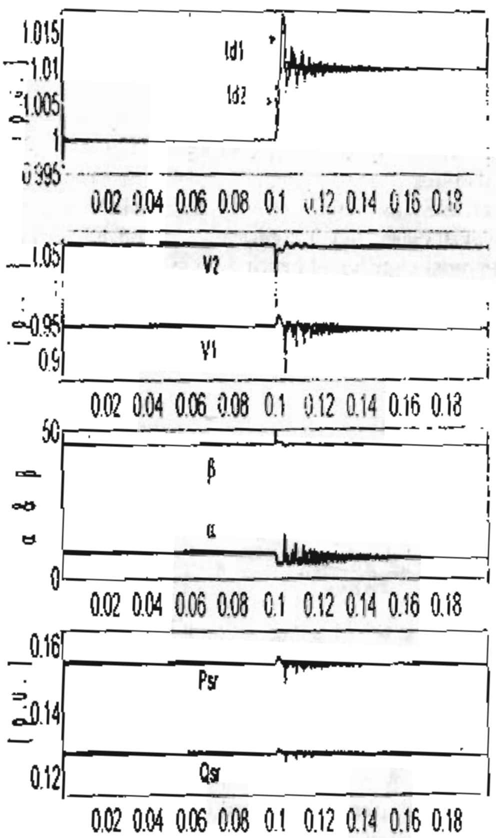

Fig (10) Time response of system variables due 0.01 increase in inverter current order (SIF adopting CDV/CC control at $ESCR_{Rect}$ 2.7776).

Fig. (11) corresponds to an unstable SIF configuration. The system adopts CC/Cβ control mode at SCR_{Inv} of 1.66091 (HP). Fig. 11.a shows the time response of AC line voltages, rectifier firing angle and static load powers at inverter bus. The variables are found to oscillate around an unstable node, which is evident from the phase plane of AC and DC line voltages against DC line current at inverter bus as shown in Fig. 11.b.

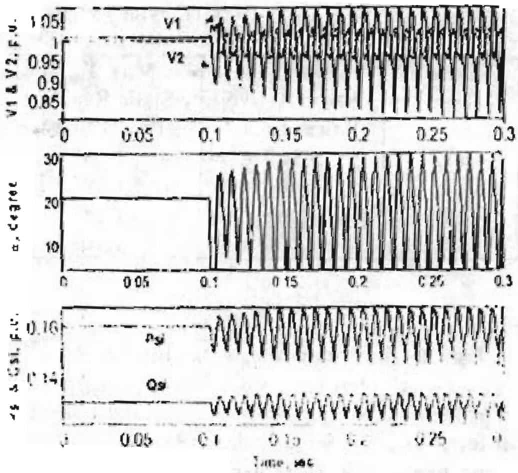

Fig 11.a Time responses

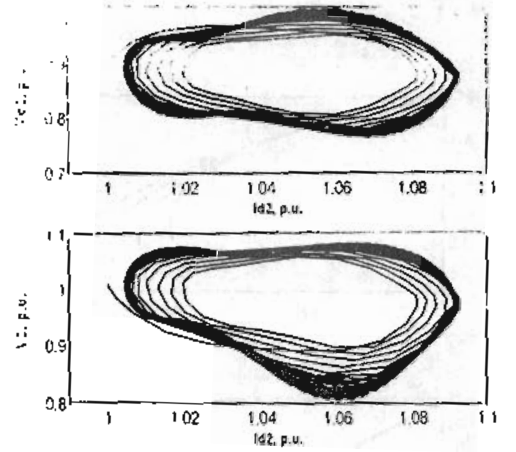

Fig 11.b Phase plane of V_{d2}, I_{d2} and V_2, I_{d2}

Fig 11 Time responses and phase planes due to 0.05 increase in rectifier current order (SIF adopting CC/Cβ at $ESCR_{Inv}$ of 1.66091)

To compare between the stability performances of SIF and SIFAC under load conditions, the responses of the later are studied at $ESCR_{Inv}$ value below that rendered the SIF configuration unstable. Fig 12 shows the phase plane of AC and DC line voltages against DC line current at inverter bus for an SIFAC configuration at $ESCR_{Inv}$ of 1.6609 which illustrates that the variables oscillate around a stable node. The system remained stable due to the active and reactive power transfer capability from rectifier bus to inverter bus through the parallel AC line, which raises the voltage at the inverter bus.

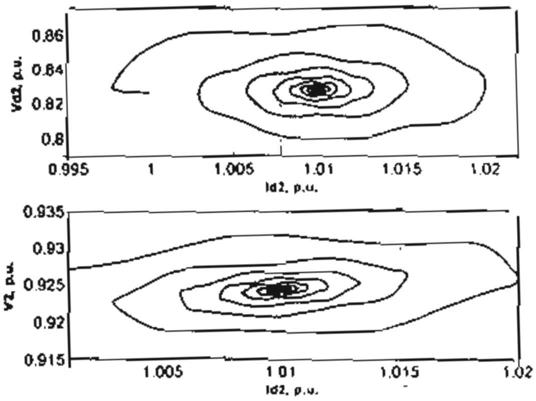

Fig. 12 Phase planes of V_{d2}, I_{d2} and V_2, I_{d2} due to 0.05 increase in rectifier current order (SIFAC adopting CC/Cβ at $ESCR_{Inv}$ of 1.6609)

The different values of critical ESCR at different control modes for both SIF and SIFAC are presented in Table 5.

Table 5 CESCR with Static Load at rectifier or inverter bus.

Control Mode	SIF	SIFAC
CDA/CC	1.89516 (SN)	1.8799 (SN)
CC/Cβ	1.66091 (HP)	1.3081 (PF)
CDV/ CC	2.6544 (PF)	1.3314 (PF)
CP/Cβ	1.7693 (HP)	1.2512 (SN)
CDV/CP	2.8248 (PF)	2.2717 (PF)

CASE (b) Dynamic and Static Load

The dynamic active and reactive load and the static load are applied at the converter bus. The load data is shown in Table 6.

Table 6 Dynamic & Static load data in p.u.

k_{pc}	n_{pv}	k_{pL}	T_p
0.05	2	0.01	0.04
k_{qc}	n_{qv}	k_{qL}	T_q
0.05	2	0.01	0.04

Fig. 13 corresponds to an unstable case with SIF configuration at SCR_{Recl} of 1.06954 (Hopf bifurcation). The system adopts CP/Cβ control mode. Fig. 13.a shows the time responses of DC line current at both rectifier and inverter sides due to a change of power order by 0.001 p.u which oscillate around an unstable node. It shows the time response of AC line voltage at inverter bus. It shows also the time response of active and reactive dynamic and static load power. The active and reactive dynamic load power is largely affected by system change rather than that of static load. Fig. 13.b shows the phase plane of AC and DC line voltages against DC line current at inverter bus which illustrates that they oscillate around an unstable node point.

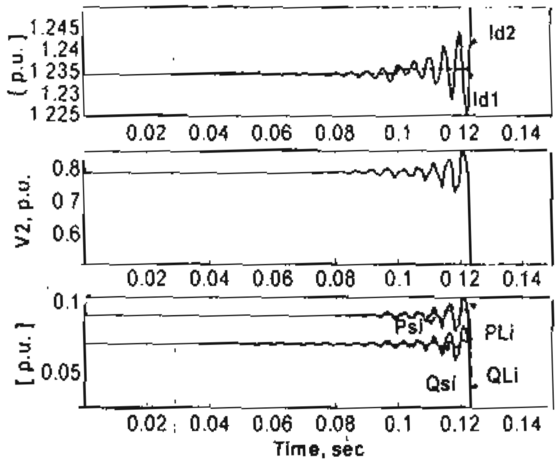

Fig 13.a Time responses due to rectifier power order increase of 0.001 (SIF adopts CP/Cβ at $ESCR_{Inv}$ 1.06954)

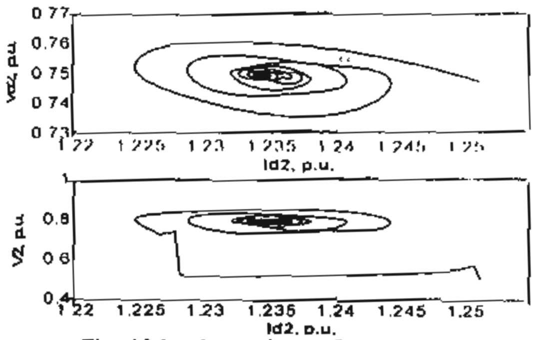

Fig. 13.b phase plane of V_{d2}, I_{d2} and V_2, I_{d2} due to rectifier power order increase of 0.001 (SIF adopts CP/Cβ at $ESCR_{Inv}$ 1.06954)

Fig. 14 corresponds to a stable case with SIFAC configurations at SCR_{Recl} of 1.7032. The system adopts CP/Cβ control mode. It shows the time responses due to a larger change of power order of 0.05 p.u.

The system variables oscillate around a stable node in spite of the larger perturbation due to the compensating effect of the AC line.

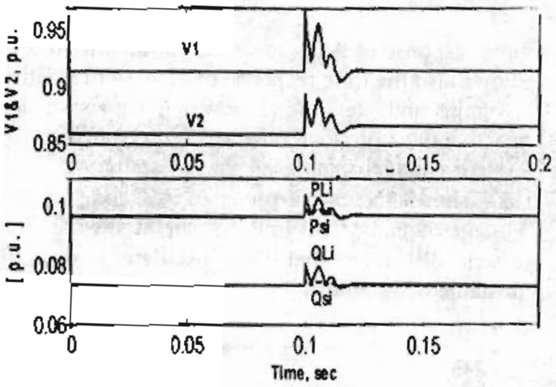

Fig 14 system variables' response due to increase of rectifier power order by 0.05 (SIFAC adopts CP/Cβ , $ESCR_{inv}$ = 1.7032)

The system's critical ESCR values at different control mode of SIF and SIFAC with dynamic and static load are presented in Table 7.

Table 7 CESCR with Static and Dynamic Loads

Control Mode	SIF	SIFAC
CDA/CC	1.8336 (SN)	1.9955 (PF)
CC/Cβ	1.5085 (HP)	1.4421 (HP+SN)
CDV/ CC	2.5351 (PF)	1.7391 (PF)
CP/Cβ	1.06954 (HP)	1.3194 (SN)
CDV/CP	2.2199 (PF)	2.8936 (PF)

IV. CONCLUSION

The effect of different types of static and dynamic loads at both rectifier and inverter terminals on the stability of the system were presented. The analysis has been carried out for different HVDC system configurations and the maximum DC power transfer at different loading conditions have been assessed. The results verified the expected negative bearing of reactive loading at inverter on stability as well as the positive effect of the AC line in SIFAC configuration. Furthermore, the analysis revealed certain operating conditions where system's stability was seemingly enhanced at the cost of de-rated system's performance; as the case of rectifier side loading. Further work is recommended to propose indices that adequately consider HVDC System's stability and performance as well.

REFERENCES

[1] Pilotto L. A. S., Szechtman M., Hammad A. E. "Transient AC Voltage Related Phenomena for HVDC Schemes Connected to Weak AC Systems", *IEEE Transactions on Power Delivery. Vol. 7, No. 3, PP. 1396-1404, July (1992)*

[2] Vijay K. Sood, "HVDC AND FACTS Controllers Applications of Static Converters in Power Systems", *Kluwer Academic Publishers, (2004).*

[3] Aik, D. L. H. and Anderson G., "Influence of Load Characteristics on The Power/Voltage Stability of HVDC Systems, Part 1: Basic Equations and Relationships", *IEEE Transactions on Power Delivery. Vol. 13, No. 4, PP.1437-1444, Oct. (1998).*

[4] Aik, D. L. H. and Anderson G., "Influence of Load Characteristics on The Power/Voltage Stability of HVDC Systems, Part 2: Stability Margin Sensitivity", *IEEE Transactions on Power Delivery. Vol. 13, No. 4, PP. 1445-1452, Oct. (1998).*

[5] Padiyar K. R. and Rao S. S., "Dynamic Analysis of Voltage in AC-DC Systems", *Elsevier Science Ltd. Electrical Power & Energy Systems, vol. 18, No. 1, PP. 11-18, (1996)*

[6] Aik, D. L. H. and Anderson G., "Nonlinear Dynamics In Hvdc Systems", *IEEE Transactions on Power Delivery. Vol. 14, No. 4, PP.1417-1426, October (1999).*

[7] Aik, D. L. H. and Anderson G., "Voltage Stability Analysis Multi-Infeed HVDC Systems", *IEEE Transactions on Power Delivery. Vol. 12, No. 3, PP. 1309, July (1997).*

[8] Lotfy A. A., Bedir I., Abed-El-Kareem M. E. and Aly G. E. M., "Dynamic Voltage Stability Analysis in HVDC Systems", Alexandria Eng. Journal, Vol. 46, No.2, *PP* 111-119, March (2007).

[9] Zhao C., and Sun Y., "Study on Control Strategies to Improve The Stability of Multi-Infeed HVDC Systems Applying VSC-HVDC", *IEEE CCECE/CCGEL, Ottawa, PP. 2253-2257 May (2005).*

[10] Pai M. A., Sauer P. W., Lesieutre B. C., and Adapa R., "Structural Stability Power System – Effect of Load Models", *IEEE Trans. on Power systems, Vol. 10, No. 2, PP. 609-615, May (1995).*

[11] Mithulananthan N., Ganizares C. A. and Reeve J., "Indices to Detect Hopf Bifurcations in Power Systems", *NAPS-2000, PP. 1-7. (2000)*

[12] Harb A. M. and Abed-Jabar N., "Controlling Hopf Bifurcations and Chaos in A Small Power Systems", *Elsevier Science Ltd. Chaos, Solutions and Fractals, 18, PP. 1055-1063, (2003)*

[13] Hranilovic S. and Canizares C. A., "Transcritical and Hopf Bifurcations in AC/DC Systems", *Prog. Bulk Power Voltage Phenomena, Davos, Switzerland, PP. 105-114, August (1994).*